Anomalous quartic $WW\gamma\gamma$ and $ZZ\gamma\gamma$ couplings in $e\gamma$ collision with initial beam and final state polarizations

S. Ataǧ* and İ. Şahin†

Department of Physics, Faculty of Sciences, Ankara University, 06100 Tandogan, Ankara, Turkey
(Received 4 July 2006; revised manuscript received 9 March 2007; published 5 April 2007)

The constraints on the anomalous quartic $WW\gamma\gamma$ and $ZZ\gamma\gamma$ gauge boson couplings are investigated through the processes $e\gamma \to W^-\gamma\nu_e$ and $e\gamma \to Z\gamma e$. Considering the longitudinal and transverse polarization states of the final W or Z boson and incoming beam polarizations we find 95% confidence level limits on the anomalous coupling parameters a_0 and a_c with an integrated luminosity of 500 fb^{-1} and $\sqrt{s} = 0.5$, 1 TeV energies. Assuming the $W^+W^-\gamma\gamma$ couplings are independent of the $ZZ\gamma\gamma$ couplings we show that the longitudinal polarization state of the final gauge boson improves the sensitivity to anomalous couplings by a factor of 2-3 depending on energy and coupling. An extra enhancement in sensitivity by a factor of 1.3 comes from a set of initial beam polarizations.

DOI: 10.1103/PhysRevD.75.073003 PACS numbers: 12.15.Ji, 12.60.Cn, 14.80.Cp

I. INTRODUCTION

Many predictions of the standard model (SM) of electroweak interactions have been tested with good accuracy in the recent experiments at CERN e^+e^- collider LEP and Fermilab Tevatron and the experimental results confirm the $SU_L(2) \times U_Y(1)$ gauge structure of SM. However, self-interactions of gauge bosons have not been tested with good accuracy and their precision measurements are in the scope of future experiments. Therefore precision measurements of these couplings in the future colliders will be the crucial test of the structure of the SM. Deviation of the couplings from the expected values would indicate the existence of new physics beyond the SM. In this work we analyzed genuinely quartic $WW\gamma\gamma$ and $ZZ\gamma\gamma$ couplings which do not induce new trilinear vertices.

In writing effective operators for genuinely quartic couplings we employ the formalism of [1]. Imposing custodial $SU(2)_{\text{Weak}}$ symmetry and local $U(1)_{\text{em}}$ symmetry and if we restrict ourselves to C and P conserving interactions, the effective Lagrangian for the $W^+W^-\gamma\gamma$ couplings is given by

$$L = L_0 + L_c, \tag{1}$$

$$L_0 = \frac{-\pi\alpha}{4\Lambda^2} a_0 F_{\mu\nu} F^{\mu\nu} W^{(i)}_\alpha W^{(i)\alpha}, \tag{2}$$

$$L_c = \frac{-\pi\alpha}{4\Lambda^2} a_c F_{\mu\alpha} F^{\mu\beta} W^{(i)\alpha} W^{(i)}_\beta, \tag{3}$$

where $W^{(i)}$ is the $SU(2)_{\text{Weak}}$ triplet and $F_{\mu\nu}$ is the electromagnetic field strength. Effective Lagrangians (2) and (3) also give rise to anomalous $ZZ\gamma\gamma$ couplings. For sensitivity calculations to anomalous couplings we set the new physics energy scale Λ to M_W. The vertex functions for $W^+(k_1^\mu)W^-(k_2^\nu)\gamma(p_1^\alpha)\gamma(p_2^\beta)$ generated from the effective Lagrangians (2) and (3) are given by

$$i\frac{2\pi\alpha}{\Lambda^2} a_0 g_{\mu\nu}[g_{\alpha\beta}(p_1 \cdot p_2) - p_{2\alpha} p_{1\beta}], \tag{4}$$

$$\begin{aligned} i\frac{\pi\alpha}{2\Lambda^2} a_c [&(p_1 \cdot p_2)(g_{\mu\alpha} g_{\nu\beta} + g_{\mu\beta} g_{\alpha\nu}) \\ &+ g_{\alpha\beta}(p_{1\mu} p_{2\nu} + p_{2\mu} p_{1\nu}) - p_{1\beta}(g_{\alpha\mu} p_{2\nu} + g_{\alpha\nu} p_{2\mu}) \\ &- p_{2\alpha}(g_{\beta\mu} p_{1\nu} + g_{\beta\nu} p_{1\mu})], \end{aligned} \tag{5}$$

respectively. For a convention, we assume that all the momenta are incoming to the vertex. The anomalous $ZZ\gamma\gamma$ couplings are obtained by multiplying (4) and (5) by $\frac{1}{\cos^2\theta_W}$ and making $W \to Z$.

Indirect information on quartic gauge boson interactions comes from the fact that they modify gauge boson two point functions at one loop [2]. The measurements at low energy and the Z pole give constraints on these couplings to be smaller than 10^{-3}–10^{-1} depending on the couplings.

Measurements at CERN e^+e^- collider LEP2 provide present collider limits on anomalous quartic $WW\gamma\gamma$ and $ZZ\gamma\gamma$ couplings. Recent results from OPAL Collaboration for $W^+W^-\gamma\gamma$ couplings are given by $-0.020\ \text{GeV}^{-2} < \frac{a_0}{\Lambda^2} < 0.020\ \text{GeV}^{-2}$, $-0.052\ \text{GeV}^{-2} < \frac{a_c}{\Lambda^2} < 0.037\ \text{GeV}^{-2}$ and for $ZZ\gamma\gamma$ couplings $-0.007\ \text{GeV}^{-2} < \frac{a_0}{\Lambda^2} < 0.023\ \text{GeV}^{-2}$, $-0.029\ \text{GeV}^{-2} < \frac{a_c}{\Lambda^2} < 0.029\ \text{GeV}^{-2}$ at 95% C.L. assuming that the $W^+W^-\gamma\gamma$ couplings are independent of the $ZZ\gamma\gamma$ couplings [3]. If it is assumed that $W^+W^-\gamma\gamma$ couplings are dependent on the $ZZ\gamma\gamma$ couplings (the same a_0 and a_c parameters are used for

*Electronic address: atag@science.ankara.edu.tr
†Electronic address: isahin@science.ankara.edu.tr

both $W^+W^-\gamma\gamma$ and $ZZ\gamma\gamma$ couplings) then the 95% C.L. sensitivity limits are improved to $+0.002\ \mathrm{GeV}^{-2} < \frac{a_0}{\Lambda^2} < 0.019\ \mathrm{GeV}^{-2}$, $-0.022\ \mathrm{GeV}^{-2} < \frac{a_c}{\Lambda^2} < 0.029\ \mathrm{GeV}^{-2}$.

Since the research and development on linear e^+e^- colliders and its operating modes of e^+e^-, $e\gamma$, and $\gamma\gamma$ [4,5] have been progressing there have been several studies of anomalous quartic gauge boson couplings through the reactions $e^+e^- \to VVV$ [6], $e^+e^- \to FFVV$ [7], $e\gamma \to VVF$ [8], $e\gamma \to VVVF$ [9], $\gamma\gamma \to VV$ [10], $\gamma\gamma \to VVV$, and $\gamma\gamma \to VVVV$ [9] where $V = Z$, W, or γ and $F = e$ or ν. These vertices have also been studied at hadron colliders via the process $pp(\bar{p}) \to \gamma\gamma Z$ or $\gamma\gamma W$ [12].

In this work we consider the processes $e\gamma \to \nu_e W\gamma$ and $e\gamma \to Ze\gamma$ to investigate $WW\gamma\gamma$ and $ZZ\gamma\gamma$ couplings. The bounds on these couplings were shown to be weaker than the other anomalous quartic couplings discussed in Ref. [8] in the $e\gamma$ collision. We take into account the cross sections for longitudinal and transverse polarization states of the final W or Z boson as well as the incoming beam polarizations to improve the bounds, assuming the polarization of W and Z can be measured [13].

II. POLARIZED REAL γ BEAM

Real gamma beam is obtained by the Compton backscattering of laser photons off a linear electron beam where most of the photons are produced at the high energy region. The luminosities for $e\gamma$ and $\gamma\gamma$ collisions turn out to be of the same order as the one for e^+e^- collision [14]. This is the reason why one gets a larger cross section for photoproduction processes with real photons.

The spectrum of backscattered photons is needed for an integrated cross section in connection with helicities of initial laser photon and electron:

$$f_{\gamma/e}(y) = \frac{1}{g(\zeta)}\Big[1 - y + \frac{1}{1-y} - \frac{4y}{\zeta(1-y)} + \frac{4y^2}{\zeta^2(1-y)^2} + \lambda_0\lambda_e r\zeta(1-2r)(2-y)\Big], \tag{6}$$

where

$$g(\zeta) = g_1(\zeta) + \lambda_0\lambda_e g_2(\zeta),$$
$$g_1(\zeta) = \Big(1 - \frac{4}{\zeta} - \frac{8}{\zeta^2}\Big)\ln(\zeta+1) + \frac{1}{2} + \frac{8}{\zeta} - \frac{1}{2(\zeta+1)^2}, \tag{7}$$

$$g_2(\zeta) = \Big(1 + \frac{2}{\zeta}\Big)\ln(\zeta+1) - \frac{5}{2} + \frac{1}{\zeta+1} - \frac{1}{2(\zeta+1)^2}. \tag{8}$$

Here $r = y/[\zeta(1-y)]$, $y = E_\gamma/E_e$, and $\zeta = 4E_eE_0/M_e^2$. E_0 is the energy of the initial laser photon and E_e and λ_e are the energy and the helicity of the initial electron beam before Compton backscattering. It is clear from $g(\zeta)$ spectrum $f(y)$ takes larger values when $\lambda_0\lambda_e$ has a negative sign. Because of this we keep this result during our computation. The maximum value of y reaches 0.83 when $\zeta = 4.8$.

The helicity of the Compton backscattered photons can be written below in terms of the same parameters given above

$$\xi(E_\gamma, \lambda_0) = \frac{\lambda_0(1-2r)(1-y+1/(1-y)) + \lambda_e r\zeta[1+(1-y)(1-2r)^2]}{1-y+1/(1-y) - 4r(1-r) - \lambda_e\lambda_0 r\zeta(2r-1)(2-y)} \tag{9}$$

which has the highest value when the parameter y is around its highest value.

III. SINGLE W OR Z BOSON PRODUCTION IN $e\gamma$ COLLISION

The single production of the W boson via the process $e\gamma \to W^-\gamma\nu_e$ is described by seven tree-level diagrams. Only the t-channel W exchange diagram contains anomalous $W^+W^-\gamma\gamma$ couplings. The helicity amplitudes have been calculated via vertex amplitude techniques [15] and the phase space integrations have been performed by GRACE [16] which uses a Monte Carlo routine. In all calculations we impose a cut on the final state photon transverse momentum $p_T^\gamma > 15$ GeV.

In this work we assume that the transverse and the longitudinal polarization states of the final W can be measured [13]. This is a reasonable assumption since the angular distributions of the decay products of the final W boson are closely related to the polarization states of it. Therefore in principle, polarization states of the final W boson can be determined by measuring the angular distributions of the W decay products. Let us consider the differential cross section for the complete process $e\gamma \to W^-\gamma\nu_e \to \ell\bar{\nu}_l\gamma\nu_e$ where the lepton channel of the W boson decay is taken into account. It can be written in the following form:

$$d\sigma(e\gamma \to W^-\gamma\nu_e \to \ell\bar{\nu}_l\gamma\nu_e) = \frac{1}{32\pi M_W\Gamma_W}\sum_{\lambda_W} d\sigma_a(\lambda_W)|M_b(\lambda_W)|^2 d\cos\theta^\star, \tag{10}$$

where λ_W and Γ_W show the polarization state and the total decay width of the W boson. $d\sigma_a(\lambda_W)$ is the helicity dependent differential cross section for the process $e\gamma \to W^-\gamma\nu_e$ and $M_b(\lambda_W)$ is the helicity amplitude for the W decay to leptons ($W^- \to l\bar{\nu}_l$) in the rest frame of W. $\theta^\star$ is the polar angle of the final state leptons $l\bar{\nu}_l$ in the W rest

frame with respect to the W-boson direction in the $l\bar{\nu}_l\gamma\nu_e$ rest frame.

Decay amplitudes $|M_b(\lambda_W)|^2$ have simple angular dependences. When we take the helicity basis ($\lambda_W = +, -, 0$) explicit forms of these amplitudes in the W rest frame are given by

$$|M_b(+)|^2 = \frac{g_W^2 M_W^2}{4}(1 - \cos\theta^\star)^2, \tag{11}$$

$$|M_b(-)|^2 = \frac{g_W^2 M_W^2}{4}(1 + \cos\theta^\star)^2, \tag{12}$$

$$|M_b(0)|^2 = \frac{g_W^2 M_W^2}{2}(\sin\theta^\star)^2, \tag{13}$$

$$|M_b(\mathrm{LO})|^2 = |M_b(0)|^2, \tag{14}$$

$$|M_b(\mathrm{TR})|^2 = |M_b(+)|^2 + |M_b(-)|^2. \tag{15}$$

By measuring the polar angle distributions of the W decay products, one can directly determine the differential cross sections for fixed W helicities. Complete factors $\frac{1}{32\pi M_W\Gamma_W}|M_b(\lambda_W)|^2$ in front of $d\sigma_a(\lambda_W)$ in differential cross sections are plotted in Fig. 1. As can be seen from Fig. 1 longitudinal (LO) and transverse (TR) distributions are well separated from each other.

The single production of the Z boson via process $e\gamma \to Z\gamma e$ is also described by seven tree-level diagrams including only one t-channel Z exchange diagram with anomalous $ZZ\gamma\gamma$ couplings. The differential cross section for the complete process $e\gamma \to Z\gamma e \to \ell^+\ell^-\gamma e$ where the lepton channel of the Z boson decay is chosen can be written in a similar way to the W case above:

$$d\sigma(e\gamma \to Z\gamma e \to \ell^+\ell^-\gamma e) = \frac{1}{32\pi M_Z\Gamma_Z}\sum_{\lambda_Z} d\sigma_a(\lambda_Z)|M_b(\lambda_Z)|^2 d\cos\theta^\star, \tag{16}$$

where $M_b(\lambda_Z)$ is the helicity dependent amplitude for the Z

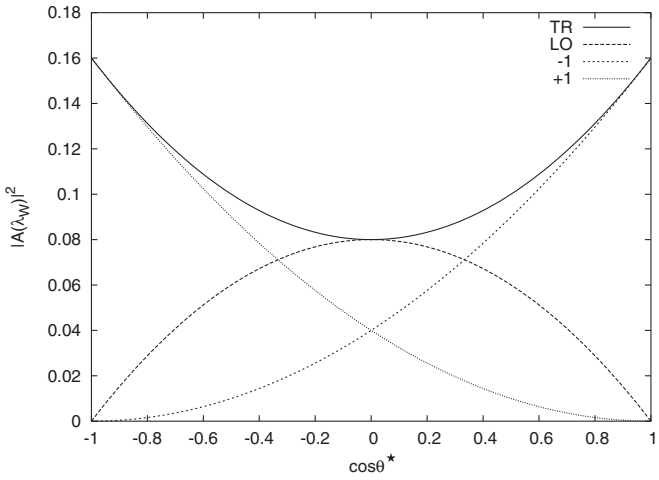

FIG. 1. Angular distribution of the W decay products of the lepton channel in the rest system of the W boson where $|A(\lambda_W)|^2 = \frac{1}{32\pi M_W\Gamma_W}|M_b(\lambda_W)|^2$. TR and LO stand for transverse and longitudinal.

decay to leptons $Z \to \ell^+\ell^-$ in the rest frame of Z. $\theta^\star$ has the same definition as the case of the W boson. The explicit form of the decay amplitudes $|M_b(\lambda_Z)|^2$ with helicity basis $\lambda_Z = +, -, 0$ in the Z rest frame are given as follows

$$|M_b(+)|^2 = \frac{M_Z^2}{2}[g_L^2(1 - \cos\theta^\star)^2 + g_R^2(1 + \cos\theta^\star)^2], \tag{17}$$

$$|M_b(-)|^2 = \frac{M_Z^2}{2}[g_L^2(1 + \cos\theta^\star)^2 + g_R^2(1 - \cos\theta^\star)^2], \tag{18}$$

$$|M_b(0)|^2 = M_Z^2(g_L^2 + g_R^2)\sin^2\theta^\star. \tag{19}$$

The behavior of $|M_b(\mathrm{TR})|^2$ and $|M_b(\mathrm{LO})|^2$ is almost the same as in Fig. 1.

The form of the helicity dependent differential cross section for the $e\gamma \to Z\gamma e$ subprocess with initial beam polarizations is

$$d\hat{\sigma}(\lambda_0, \lambda_Z) = \{\tfrac{1}{4}(1 - P_e)[(1 + \xi(E_\gamma, \lambda_0))|M(+, L; \lambda_Z, L)|^2 + (1 - \xi(E_\gamma, \lambda_0))|M(-, L; \lambda_Z, L)|^2] + \tfrac{1}{4}(1 + P_e)[(1 + \xi(E_\gamma, \lambda_0))|M(+, R; \lambda_Z, R)|^2 + (1 - \xi(E_\gamma, \lambda_0))|M(-, R; \lambda_Z, R)|^2]\}(PS), \tag{20}$$

where helicity amplitudes $M(\lambda_\gamma, \sigma_e; \lambda_Z, \sigma_e')$ are defined to represent both incoming and outgoing electron helicities σ_e: L, R and σ_e': L, R together with incoming and outgoing boson helicities λ_γ: $+ -$, λ_Z: $+ -0$. The polarization index of the outgoing photon is not shown in the amplitude due to the sum over its polarization. The phase space and initial flux factors are included in (PS). The above cross section has been connected to initial laser photon helicity λ_0 before Compton backscattering. P_e is the initial electron beam polarization and is different from λ_e which refers to a different beam. The information about the incoming photon beam polarization $\xi(E_\gamma, \lambda_0)$

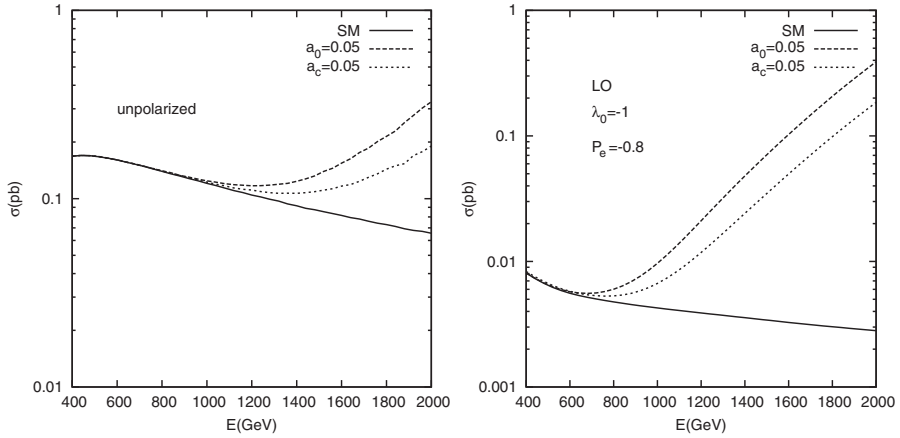

FIG. 2. The total cross sections of $e\gamma \to Z\gamma e$ as a function of collider energy for the SM and the anomalous couplings $a_0 = 0.05$, $a_c = 0.05$ with the unpolarized and longitudinally polarized (LO) final Z boson with polarized incoming beams. Only one of the anomalous couplings is kept different from their SM value.

(Compton backscattered photons) can be found in the previous section. In the case of W production the last two terms beginning with $(1 + P_e)$ will vanish.

The expression of the integrated cross section over the backscattered photon spectrum is written below for completeness:

$$d\sigma(\lambda_0, \lambda_Z) = \int_{y_{\min}}^{y_{\max}} f_{\gamma/e}(y) d\hat{\sigma}(\lambda_0, \lambda_Z) dy \qquad (21)$$

with $y_{\min} = M_Z^2/s$. Here $\hat{s}$ is related to s, the square of the center of mass energy of the e^+e^- system, by $\hat{s} = ys$.

In order to get an idea about the influence of the initial and final state polarizations on the cross section with anomalous $ZZ\gamma\gamma$ and $WW\gamma\gamma$ couplings we give a set of figures. In all figures we take into account the polarization configuration which gives the largest deviation from the standard model when compared to unpolarized cases. This configuration corresponds to $\lambda_0 = -1$, $P_e = -0.8$, and longitudinal polarization of the final state Z or W boson. In all calculations λ_e has been chosen to satisfy $\lambda_0\lambda_e < 0$ to increase the cross section. One can see from Fig. 2 the deviations of the total cross sections for the anomalous $ZZ\gamma\gamma$ couplings $a_0 = 0.05$ and $a_c = 0.05$ from their SM value as a function of center-of-mass energy $\sqrt{s}$ of the e^-e^+ system. Only one of the anomalous couplings is kept different from the SM value. From these figures, it is clear that the longitudinal polarization remarkably improves the deviations from the SM at increasing energies when compared to the unpolarized case. The transverse polarization is ineffective on the variation of the cross section for the given anomalous coupling values. Therefore, the curves related to transverse polarization are not given. The cross section of the process $e\gamma \to W^-\gamma\nu_e$ with anomalous $WW\gamma\gamma$ couplings shows the similar features as a function of energy.

In Figs. 3 and 4 the total cross sections for $e\gamma \to W^-\gamma\nu_e$ and $e\gamma \to Z\gamma e$ as a function of anomalous couplings a_0

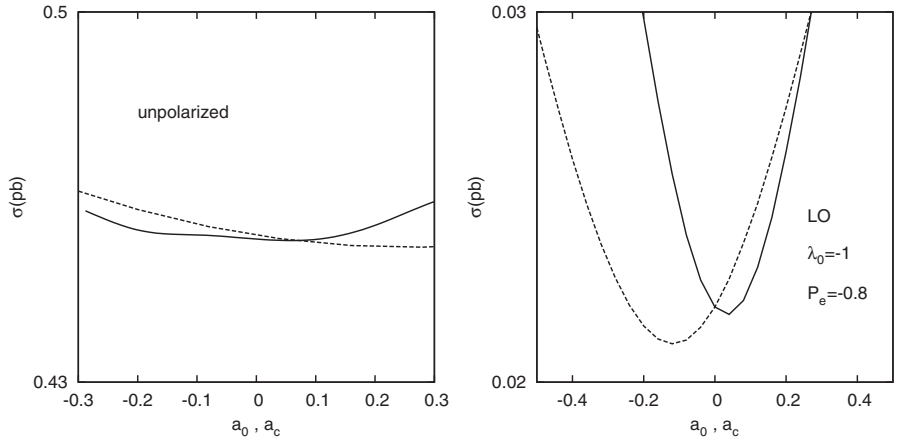

FIG. 3. The total cross sections of $e\gamma \to W^-\gamma\nu_e$ as a function of anomalous couplings a_0 and a_c for the unpolarized and longitudinally polarized final W boson with incoming beam polarizations at the main e^+e^- collider energy $\sqrt{s} = 0.5$ TeV. Solid curves show the behavior against the coupling a_0. y axes are the logarithmic scale.

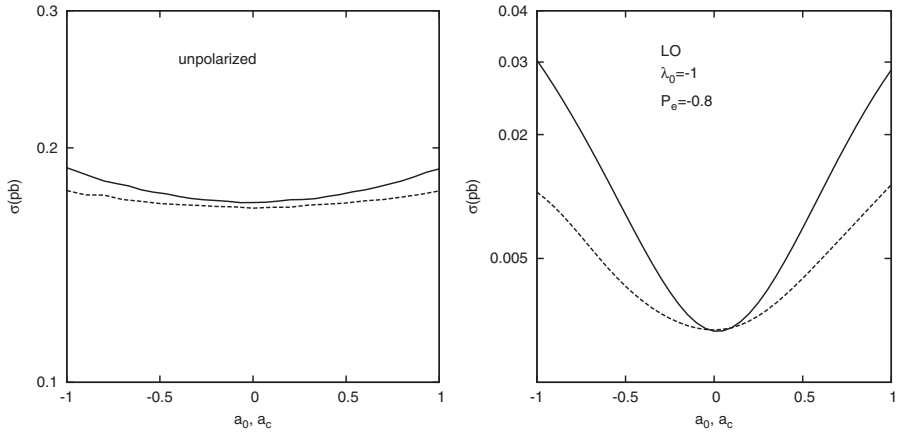

FIG. 4. The total cross sections of $e\gamma \to Z\gamma e$ as a function of anomalous couplings a_0 and a_c for the unpolarized and longitudinally polarized final Z boson with polarized incoming beams at the main e^+e^- collider energy $\sqrt{s} = 0.5$ TeV. Solid curves show the behavior against the coupling a_0.

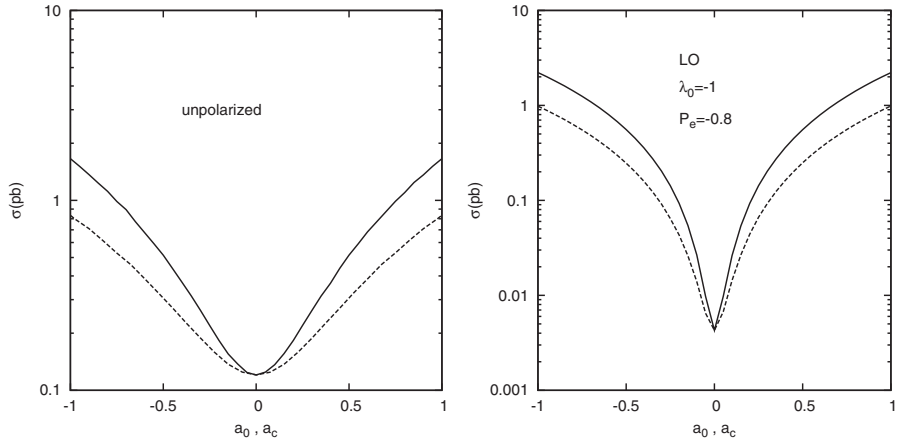

FIG. 5. The same as Fig. 4 but for the energy $\sqrt{s} = 1$ TeV.

and a_c are plotted for the above mentioned polarization configuration of the incoming beams and final state W or Z bosons at the energy $\sqrt{s} = 0.5$ TeV. Here, we assume that the anomalous $W^+W^-\gamma\gamma$ couplings are independent of the $ZZ\gamma\gamma$ couplings. The same curves are given in Fig. 5 for $e\gamma \to Z\gamma e$ at the collider energy $\sqrt{s} = 1$ TeV.

From Figs. 3 and 4 it is clear that longitudinally polarized cross sections seem highly sensitive to anomalous couplings. Figure 5 shows that anomalous couplings become far more effective as the energy increases. In all figures we realize the fact that a_0 dependence of the cross sections causes more separation from the SM. The comparison of the other polarization configurations to unpolarized cases and to each other will be given in the following section.

IV. LIMITS ON THE ANOMALOUS COUPLINGS

For a concrete result, 95% C.L. limits on the anomalous coupling parameters a_0 and a_c have been obtained using χ^2 analysis at $\sqrt{s} = 0.5$, 1 TeV and integrated luminosity $L_{\text{int}} = 500$ fb^{-1} without systematic errors. In order to get realistic results the number of events are given as $N = AL_{\text{int}}\sigma BR$ where A is the overall acceptance and BR is the branching ratio of the W and Z boson for the leptonic channel. The limits for the anomalous $WW\gamma\gamma$ couplings are given in Table I for unpolarized, transverse, and longitudinal polarization states of the final W boson and several combinations of incoming beams polarizations with the acceptance $A = 0.85$. In Tables II and III the limits for the anomalous $ZZ\gamma\gamma$ couplings are given for more polarization configurations based on the fact that fermion-fermion-Z coupling has both left and right-handed parts. One can see from Table I that longitudinal polarization together with the initial beam polarizations improves limits at least by a factor of 2-3 for a_0 and a factor of 2 for a_c at $\sqrt{s} = 0.5$ TeV. This improvement reaches the limits by a factor of 3-4 for a_0 but by a factor of 2-2.6 for a_c at $\sqrt{s} = 1$ TeV energy. An increase in energy from 0.5 TeV to 1 TeV improves the limits by a factor of 8 in the longitudi-

TABLE I. Sensitivity of the $e\gamma$ collision to $WW\gamma\gamma$ couplings at 95% C.L. for $\sqrt{s} = 0.5$, 1 TeV and $L_{\text{int}} = 500\ \text{fb}^{-1}$. The effects of the final state W boson polarization and initial beam polarizations are shown in each row. Here λ_0 is the laser photon polarization before Compton backscattering and P_e electron beam polarization. Only one of the couplings is assumed to deviate from the SM at a time. LO and TR stand for longitudinal and transverse.

$\sqrt{s}$ TeV	λ_0	P_e	λ_W	a_0	a_c
0.5	0	0	TR + LO	−0.26, 0.23	−0.20, 0.69
0.5	0	0	LO	−0.16, 0.07	−0.08, 0.32
0.5	0	0	TR	−0.49, 1.30	−0.3, 0.4 and 2.6, 3.2
0.5	1	−0.8	TR + LO	−0.20, 0.20	−0.13, 0.60
0.5	−1	−0.8	TR + LO	−0.17, 0.18	−0.10, 0.21 and 0.29, 0.65
0.5	1	−0.8	LO	−0.10, 0.06	−0.06, 0.27
0.5	1	−0.8	TR	−0.5, 1.25	−0.29, 0.38 and 1.40, 2.00
0.5	−1	−0.8	LO	−0.12, 0.05	−0.05, 0.29
0.5	−1	−0.8	TR	−0.66, 1.20	−0.15, 0.25 and 2.45, 3.00
1	0	0	TR + LO	−0.04, 0.04	−0.03, 0.07
1	0	0	LO	−0.02, 0.01	−0.01, 0.04
1	0	0	TR	−0.17, 0.34	−0.10, 0.61
1	1	−0.8	TR + LO	−0.03, 0.03	−0.03, 0.04
1	−1	−0.8	TR + LO	−0.03, 0.03	−0.03, 0.07
1	1	−0.8	LO	−0.01, 0.01	−0.01, 0.03
1	1	−0.8	TR	−0.20, 0.35	−0.09, 040.
1	−1	−0.8	LO	−0.01, 0.01	−0.01, 0.03
1	−1	−0.8	TR	−0.34, 0.33	−0.05, 0.5

nally polarized and unpolarized case. For the energies 1.5 TeV and higher, the improvement due to longitudinal polarization is expected to be much better than the unpolarized case. Tables II and III show similar features but with slightly worse limits, 2-2.6 depending on the polarizations and energy for $ZZ\gamma\gamma$ couplings. From these three tables, we realize that the improvement factor caused by initial beam polarizations alone is at most 1.3.

For $ZZ\gamma\gamma$ couplings the best limit comes from the process $\gamma\gamma \to ZZ$ due to the absence of the tree-level SM background [10]. The bounds on the anomalous $WW\gamma\gamma$ couplings have the same order as the ones from

TABLE II. Sensitivity of the $e\gamma$ collision to $ZZ\gamma\gamma$ couplings at 95% C.L. for $\sqrt{s} = 0.5$ TeV and $L_{\text{int}} = 500\ \text{fb}^{-1}$. The effects of the final state Z boson polarization and initial beam polarizations are shown in each row. Only one of the couplings is assumed to deviate from the SM at a time.

$\sqrt{s}$ TeV	λ_0	P_e	λ_Z	a_0	a_c
0.5	0	0	TR + LO	−0.50, 0.50	−0.70, 0.70
0.5	0	0	LO	−0.20, 0.30	−0.40, 0.40
0.5	0	0	TR	−1.70, 1.20	−1.80, 1.80
0.5	1	−0.8	TR + LO	−0.44, 0.42	−0.56, 0.64
0.5	−1	−0.8	TR + LO	−0.37, 0.36	−0.54, 0.60
0.5	1	0.8	TR + LO	−0.43, 0.43	−0.64, 0.65
0.5	−1	0.8	TR + LO	−0.45, 0.45	−0.60, 0.65
0.5	1	−0.8	LO	−0.21, 0.24	−0.34, 0.30
0.5	1	−0.8	TR	−1.60, 1.42	−1.00, 1.70
0.5	−1	−0.8	LO	−0.19, 0.24	−0.31, 0.29
0.5	−1	−0.8	TR	−1.60, 1.21	−1.25, 1.50
0.5	1	0.8	LO	−0.21, 0.25	−0.34, 0.32
0.5	1	0.8	TR	−1.75, 1.45	−1.35, 1.75
0.5	−1	0.8	LO	−0.23, 0.27	−0.36, 0.32
0.5	−1	0.8	TR	−1.79, 1.52	−1.29, 1.87

TABLE III. Sensitivity of the $e\gamma$ collision to $ZZ\gamma\gamma$ couplings at 95% C.L. for $\sqrt{s} = 1$ TeV and $L_{\text{int}} = 500\ \text{fb}^{-1}$. The effects of the final state Z boson polarization and initial beam polarizations are shown in each row. Only one of the couplings is assumed to deviate from the SM at a time.

$\sqrt{s}$ TeV	λ_0	P_e	λ_Z	a_0	a_c
1	0	0	TR + LO	−0.05, 0.05	−0.07, 0.07
1	0	0	LO	−0.02, 0.02	−0.03, 0.03
1	0	0	TR	−0.30, 0.30	−0.30, 0.30
1	1	−0.8	TR + LO	−0.04, 0.04	−0.05, 0.05
1	−1	−0.8	TR + LO	−0.04, 0.04	−0.06, 0.06
1	1	0.8	TR + LO	−0.04, 0.04	−0.06, 0.06
1	−1	0.8	TR + LO	−0.04, 0.04	−0.06, 0.06
1	1	−0.8	LO	−0.02, 0.02	−0.03, 0.03
1	1	−0.8	TR	−0.37, 0.34	−0.23, 0.26
1	−1	−0.8	LO	−0.02, 0.02	−0.03, 0.03
1	−1	−0.8	TR	−0.37, 0.34	−0.26, 0.29
1	1	0.8	LO	−0.02, 0.02	−0.03, 0.03
1	1	0.8	TR	−0.40, 0.39	−0.27, 0.30
1	−1	0.8	LO	−0.02, 0.02	−0.03, 0.03
1	−1	0.8	TR	−0.37, 0.34	−0.24, 0.29

the process $\gamma\gamma \to WW$ [10]. As can be seen from the references given in the introduction, the limits obtained in this work for the longitudinal cases are better than the other basic leptonic and hadronic colliders such as the linear e^+e^- collider and CERN LHC.

[1] M. Kuroda, F. M. Renard, and D. Schildknecht, Phys. Lett. B **187**, 366 (1987); G. Belanger and F. Boudjema, Phys. Lett. B **288**, 210 (1992).

[2] A. Brunstein, O. J. P. Eboli, and M. C. Gonzalez-Garcia, Phys. Lett. B **375**, 233 (1996); S. Alam, S. Dawson, and R. Szalapski, Phys. Rev. D **57**, 1577 (1998).

[3] G. Abbiendi *et al.* (OPAL Collaboration), Phys. Rev. D **70**, 032005 (2004).

[4] C. Akerlof, Ann Arbor Report No. UM HE 81-59, 1981.

[5] T. L. Barklow, in *Proceedings of the 1990 Summer Study on Research Directions for the Decade, Snowmass, Colorado, 1990* (SLAC Report No. SLAC-PUB-5364, 1990).

[6] V. Barger and T. Han, Phys. Lett. B **212**, 117 (1988); V. Barger, T. Han, and R. J. N. Philips, Phys. Rev. D **39**, 146 (1989); A. Tofighi-Niaki and J. F. Gunion, *ibid.* **39**, 720 (1989); G. Belanger and F. Boudjema, Phys. Lett. B **288**, 201 (1992); G. A. Leil and W. J. Stirling, J. Phys. G **21**, 517 (1995); O. Eboli, M. C. Gonzalez-Garcia, and J. K. Mizukoshi, Phys. Rev. D **58**, 034008 (1998); T. Han, H. He, and C. P. Yuan, Phys. Lett. B **422**, 294 (1998).

[7] E. Boos *et al.*, Phys. Rev. D **57**, 1553 (1998); **61**, 077901 (2000).

[8] O. J. P. Eboli, M. C. Gonzalez-Garcia, and S. F. Novaes, Nucl. Phys. **B411**, 381 (1994).

[9] O. J. P. Eboli and J. K. Mizukoshi, Phys. Rev. D **64**, 075011 (2001).

[10] G. Belanger and F. Boudjema, Phys. Lett. B **288**, 210 (1992).

[11] O. J. P. Eboli, M. B. Magro, P. G. Mercadante, and S. F. Novaes, Phys. Rev. D **52**, 15 (1995).

[12] O. J. P. Eboli, M. C. Gonzalez-Garcia, S. M. Lietti, and S. F. Novaes, Phys. Rev. D **63**, 075008 (2001).

[13] G. Abbiendi *et al.* (OPAL Collaboration), Eur. Phys. J. C **19**, 229 (2001).

[14] I. F. Ginzburg *et al.*, Nucl. Instrum. Methods **205**, 47 (1983); **219**, 5 (1984).

[15] A. Ballestrero and E. Maina, Phys. Lett. B **350**, 225 (1995).

[16] T. Kaneko in *New Computing Techniques in Physics Research*, edited by D. Perret-Gallix and W. Wojcik (Edition du CNRS, Paris, 1990); MINAMI-TATEYA Group, KEK Report No. 92-19, 1993; F. Yuasa *et al.*, Prog. Theor. Phys. Suppl. **138**, 18 (2000).